Thermodynamic modeling of the Nb−B system

Rockfeller Maciel Peçanha [a], Flávio Ferreira [b,*], Gilberto Carvalho Coelho [a], Carlos Angelo Nunes [a], Bo Sundman [c]

[a] *Departamento de Engenharia de Materiais, DEMAR-EEL-USP, CP116, 12600-970, Lorena, SP, Brazil*
[b] *Escola de Engenharia Industrial Metalúrgica de Volta Redonda−UFF−TMC, Av. dos Trabalhadores, 420, CEP 27255-125, Volta Redonda, RJ, Brazil*
[c] *Division of Physical Metallurgy, Royal Institute of Technology, S-10044, Stockholm 70, Sweden*

Abstract

In the present work, the Nb−B binary system was thermodynamically optimized. The stable phases in this system are BCC (niobium), Nb_3B_2, NbB, Nb_3B_4, Nb_5B_6, NbB_2, B (boron) and liquid L. The borides Nb_3B_2, NbB, Nb_3B_4 and Nb_5B_6 and the B (boron) were modeled as stoichiometric phases and the liquid L, BCC (niobium) and NbB_2 as solutions, using the sublattices model, with their excess terms described by the Redlich−Kister polynomials. The Gibbs energy coefficients were optimized based on the experimental values of enthalpy of formation, low temperature specific heat, liquidus temperatures and temperatures of invariant transformations. The calculated Nb−B diagram reproduces well the experimental values from the literature.

Keywords: A. Intermetallics, miscellaneous; B. Phase diagrams; B. Thermodynamic and thermochemical properties; E. Phase diagram, prediction

1. Introduction

The development of new high-temperature materials is essential for future generations of both aircraft engines and land-based gas turbines. Nb-silicide-based composites are potential alloy candidates because they present a good balance of properties required for high-temperature applications [1,2]. Among the information for alloy design and potential evaluation for use as structural material, the phase equilibrium is one of the most important. The present thermodynamic optimization of the Nb−B system is part of a research project, which studies the phase relations in the Nb-rich corner of the Nb−Si−B system.

The currently accepted Nb−B phase diagram [3], shown in Fig. 1, presents the following stable phases: BCC (niobium), Nb_3B_2, NbB, Nb_3B_4, Nb_5B_6, NbB_2, B (boron) and liquid L. This phase diagram is mainly based on the experimental data of Nowotny et al. [4] and shows some divergences with the diagram proposed by Rudy and Windisch [5], which is shown in Fig. 2. The main divergences are (i) Massalski proposes a peritectic formation for the Nb_3B_2, while Rudy and Windisch suggest that this phase is formed peritectoidically; (ii) Massalski proposes the stability of Nb_5B_6, based on results reported by Bolmgren and Lundström [6], while Rudy and Windisch do not mention the presence of this phase in the microstructures of their samples; (iii) Massalski proposes a homogeneity range for NbB_2 much wider than the 65−70 at% B reported in Refs. [5,7−9]; and (iv) Massalski suggests the composition of the liquid in the B-rich eutectic to be located at approximately 90 at% B, while Rudy and Windisch propose 98 at% B. To solve these discrepancies, an experimental re-investigation of the Nb−B system was performed by Borges et al. [10,11], which confirmed the stability of Nb_5B_6 and the phase relation in the Nb-rich region proposed by Rudy and Windisch, except for the composition of the liquid in

* Corresponding author. Tel.: +55 24 3344 3013; fax: +55 24 3344 3020.
E-mail address: flavio@metal.eeimvr.uff.br (F. Ferreira).

doi:10.1016/j.intermet.2006.10.054

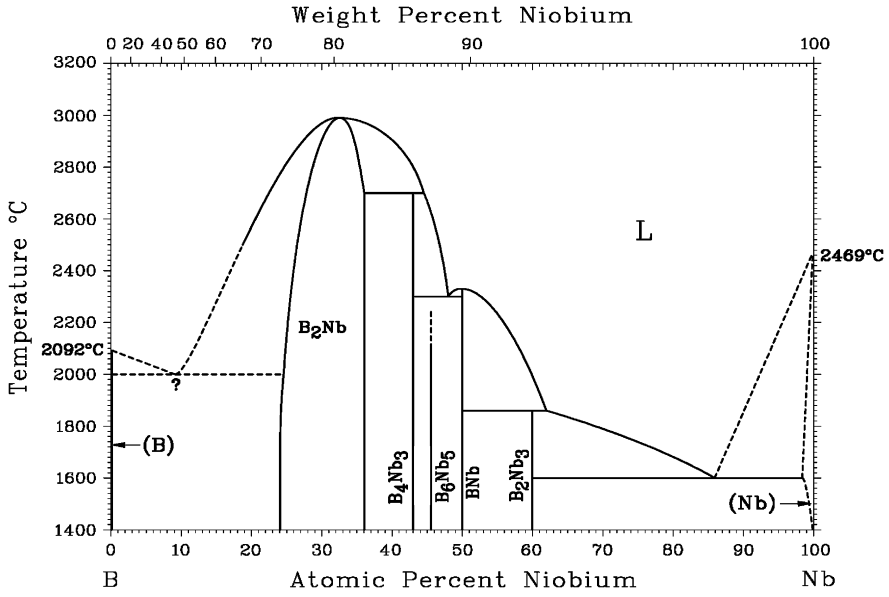

Fig. 1. Nb−B phase diagram, as assessed by Massalski [3].

the Nb-rich eutectic, located at 16 at% B instead of at 19 at% B. The composition of the B-rich eutectic was informed to be above 96 at% B.

The experimental phase diagram data available in the literature for this system are (i) the congruent melting points of NbB_2 [4,5,12] and NbB [4,5]; (ii) the temperatures and compositions of the phases for the invariant reactions [4,5,10]; and (iii) the solubility range of the phase NbB_2 [4,5,7,9,10].

The thermodynamic data available for this system are (i) the entropy of NbB_2 [13], Nb_3B_2, NbB and Nb_3B_4 phases [14]; (ii) the enthalpy of formation of NbB_2 [15−19]; and (iii) the temperature dependence of the enthalpy, $H(T) - H(298\ \mathrm{K})$, for the phases Nb_3B_2, NbB, Nb_3B_4 and NbB_2 in the 1200−2350 K range [20].

The only optimization of the Nb−B system available in the literature is due to Kaufman et al. [21]. In the modeling of the Me−Si−B systems, we have been using the Stable Element Reference (SER), adopted by the SGTE (Scientific Group Thermodata Europe) in their databases, which is not compatible with the reference state adopted by Kaufman. Furthermore, in Kaufman's work on the Nb−B system: (i) all solid phases are modeled as stoichiometric; (ii) the stability of the phase Nb_5B_6 is not considered; (iii) NbB is predicted to be formed peritectically; and (iv) more recent experimental information [6,9−11,19] were not considered. Therefore, the aim of the present work is to provide a new set of thermodynamic coefficients for the Nb−B system.

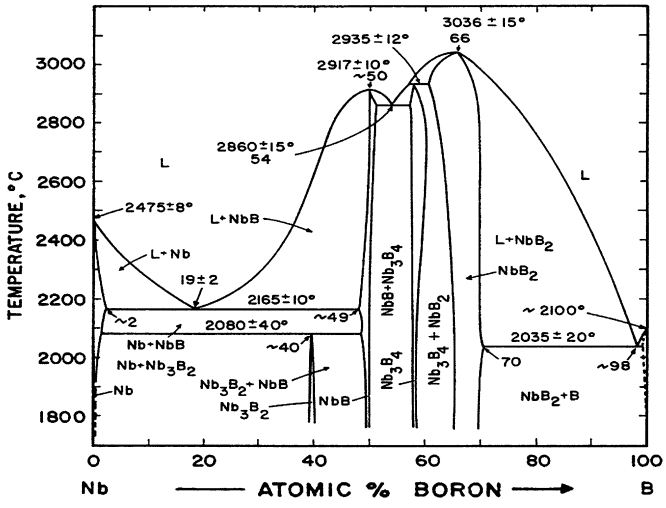

Fig. 2. Nb−B phase diagram proposed by Rudy and Windisch [5].

2. Thermodynamic models

The Nb−B phase diagram proposed by Rudy and Windisch (Fig. 2) is plotted with all intermetallic phases showing some solubility of Nb and B in their crystal structures. Except for the NbB_2, there are no quantitative experimental evidences for these phase boundaries, which would allow their modeling as solution phases. Therefore, the borides Nb_3B_2, NbB, Nb_3B_4 and Nb_5B_6 and the B (boron) were modeled as stoichiometric phases and the liquid L, BCC (niobium) and NbB_2 as solution phases, using the Compound Energy Formalism (CEF).

The CEF is described in detail by Sundman and Ågren [22] as well as by Hillert [23]. It allows an adequate description of the thermodynamic properties of phases taking the existence of sublattices into account. The sublattices are basically given by the different Wyckoff positions of the atoms in the crystal structure of the phase. Empty positions are also considered as sublattices if they are eventually occupied by atoms such as in interstitial solutions. A helpful reference for modeling intermetallic compounds is the compilation of Villars and Calvert [24]. Table 1 shows the crystal structure data of the stable solid phases in the Nb−B system, in their ideal stoichiometry [24,25]. A phase is modeled as a stoichiometric compound when it exists in a very limited composition range,

for example close to its ideal stoichiometry, and therefore one may consider each sublattice being always occupied by a unique component. When a phase exists over a not negligible composition range, the knowledge of the specific lattice defect structure is essential for the correct choice of the model, which is the case of the NbB_2 compound in the present work. In such a case, a random mixture of species, which includes vacancies, occurs in at least one of the phase sublattices. Stable or metastable end-member compounds are formed in the limiting cases of occupation of the solution sublattices. Considering the case where the species are not complex constituents such as ions, the Gibbs energy for each individual phase ϕ, G_m^{ϕ}, is described by the CEF with the following equation expressed per mole of formula unity [23] (note that the upper suffix "s" is not a power and its meaning will become clear later in the text):

$$G_m^{\phi} = \sum_s n^s \left(1 - y_{Va}^s\right) \sum_i x_i {}^oG_i^{stst} + \sum_{end} \Delta_f {}^oG_{end}^{\phi} \Pi y_i^s + RT \sum_s n^s \sum_i y_i^s \ln\left(y_i^s\right) + {}^EG_m^{\phi} \quad (1)$$

which can also be written in the form as shown below [22]

$$G_m^{\phi} = \sum_{end} {}^oG_{end}^{\phi} \Pi y_i^s + RT \sum_s n^s \sum_i y_i^s \ln\left(y_i^s\right) + {}^EG_m^{\phi} \quad (2)$$

with

$${}^oG_{end}^{\phi} = \Delta_f {}^oG_{end}^{\phi} + \sum_i {}^oG_i^{stst} n^s \quad (3)$$

The symbols in Eqs. (1)−(3) have the following meaning:

n^s is the stoichiometric coefficient of sublattice "s";
y_{Va}^s is the site fraction of vacancy in the sublattice "s";
x_i is the mole fraction of component "i" in the compound;
${}^oG_i^{stst}$ is the Gibbs free energy of component "i" at standard state;
end is an array with "end-member compounds";
$\Delta_f {}^oG_{end}^{\phi}$ is the Gibbs free energy of formation of an end-member of phase ϕ;
y_i^s is the site fraction of component "i" in the sublattice "s";
${}^EG_m^{\phi}$ is the excess Gibbs energy of phase ϕ.

The summations are performed for arrays whose elements are sublattices (s), components (i) or end-members (end), and the product Πy_i^s contains the site fractions corresponding to the components present in each end-member. As mentioned before, the end-members are formed when each sublattice is occupied by a single component at a time. Therefore, the first right-hand term of Eq. (2) describes a surface of reference in which the interaction energies between neighboring components in different sublattices are essentially considered. The second right-hand term of Eq. (2) accounts for the ideal entropy of mixing, under the assumption of random mixing of components within the solution sublattices. The excess term basically takes into account the interaction energies between different components in the solution sublattices, which are given by interaction parameters L_{xs}^{ϕ}. A general expression for the excess term is given in Ref. [22]. For the present

Table 1
Crystal structure data of the stable solid phases in the Nb−B system [24,25]

Phase	Prototype	Space group	Pearson symbol	Wyckoff position	Atom	x	y	z
BCC	W	*Im*-3*m*	*cI*2	2a	Nb	0	0	0
				6b	ip[a]	0	0.5	0.5
Nb_3B_2	U_3Si_2	*P*4/*mbm*	*tP*10	2a	Nb	0	0	0
				4g	B	0.389	0.889	0
				4h	Nb	0.181	0.681	0.5
NbB	CrB	*Cmcm*	*oC*8	4c	B	0	0.4360	0.25
				4c	Nb	0	0.1453	0.25
Nb_5B_6[b]	V_5B_6	*Cmmm*	*oC*22	2a	Nb	0	0	0
				4g	Nb	0.3855	0	0
				4h	Nb	0.1943	0	0.5
				4h	B	0.0832	0	0.5
				4g	B	0.2734	0	0
				4h	B	0.4603	0	0.5
Nb_3B_4	Ta_3B_4	*Immm*	*oI*14	2c	Nb	0.5	0.5	0
				4g	Nb	0	0.180	0
				4g	B	0	0.375	0
				4h	B	0	0.444	0.5
NbB_2	AlB_2	*P*6/*mmm*	*hP*3	1a	Nb	0	0	0
				2d	B	0.3333	0.6667	0.5
B-Rhom	B	*R*-3*m*	*hR*111	–[c]	B	–	–	–

[a] ip stands for octahedral interstitial positions.
[b] Data taken from Ref. [25].
[c] Wyckoff positions and their coordinates were intentionally suppressed for B-Rhom. The complete list can be found in Ref. [24].

work, it is sufficient to take the case of interaction energies within "excess solutions" formed under the consideration of mixing of different components "*i*1" and "*i*2" in each solution sublattice at a time while the other sublattices are occupied by single components "*i*". Using Redlich−Kister polynomials for the interaction parameters [26], the excess term may be described by:

$$^{E}G_{\mathrm{m}}^{\phi} = \sum_{\mathrm{xs}} \Pi y_i^{s} \sum_{v} {}^{v}L_{\mathrm{xs}}^{\phi}\left(y_{i1}^{s} - y_{i2}^{s}\right)^{v} \tag{4}$$

where $^{v}L_{\mathrm{xs}}^{\phi}$ is the interaction parameter of order "*v*". The first summation is performed for an array whose elements are all possible "excess solutions" (xs) and the product Πy_i^{s} contains the site fractions corresponding to the components present in each "excess solution".

2.1. Gibbs energy for pure components

The temperature dependent Gibbs energy of each pure element is described by an equation of the general form:

$$^{o}G_{\mathrm{m}}^{\phi} - H_i^{\mathrm{SER}} = a + bT + cT\ln(T) + dT^2 + eT^3 + fT^{-1} \tag{5}$$

where H_i^{SER} is the enthalpy of stable element "*i*" at 298.15 K.

2.2. Solution phase liquid

The liquid phase was modeled as a single sublattice substitutional solution. Therefore, the site fractions in Eq. (2) are equivalent to the molar fractions and the end-members are coincident with the pure elements, i.e. $^{o}G_{\mathrm{end1}}^{\mathrm{L}} = {}^{o}G_{\mathrm{Nb}}^{\mathrm{L}}$ and $^{o}G_{\mathrm{end2}}^{\mathrm{L}} = {}^{o}G_{\mathrm{B}}^{\mathrm{L}}$, yielding the following expression for its Gibbs free energy:

$$\begin{aligned} G_{\mathrm{m}}^{\mathrm{L}} = {} & x_{\mathrm{Nb}}\,{}^{o}G_{\mathrm{Nb}}^{\mathrm{L}} + x_{\mathrm{B}}\,{}^{o}G_{\mathrm{B}}^{\mathrm{L}} + RT\left[x_{\mathrm{Nb}}\ln(x_{\mathrm{Nb}}) + x_{\mathrm{B}}\ln(x_{\mathrm{B}})\right] \\ & + x_{\mathrm{Nb}}x_{\mathrm{B}}\left[{}^{0}L_{\mathrm{Nb,B}}^{\mathrm{L}} + {}^{1}L_{\mathrm{Nb,B}}^{\mathrm{L}}(x_{\mathrm{B}} - x_{\mathrm{Nb}}) + {}^{2}L_{\mathrm{Nb,B}}^{\mathrm{L}}(x_{\mathrm{B}} - x_{\mathrm{Nb}})^{2}\right] \end{aligned} \tag{6}$$

2.3. Solution phase BCC

The Body Centered Cubic (BCC) crystal structure may be modeled as a phase with two sublattices, namely the sublattice corresponding to Wyckoff positions 2a (substitutional) and that corresponding to octahedral interstitial positions 6b (Table 1). Due to compatibility reasons within thermodynamic databases, this model is usually adopted even if no interstitial solution is formed in the specific system. For the BCC phase in the Nb−B system there is no experimental information about the type of solution of B, whether interstitial or substitutional. However, it is known that the boron atoms occupy the interstitial sublattice in metals of BCC structure like Nb [27]. Therefore, also for the Nb−B system, the model $(\mathrm{Nb})(\mathrm{B,Va})_3$ was chosen yielding the following expression for its Gibbs energy:

$$\begin{aligned} G_{\mathrm{m}}^{\mathrm{BCC}} = {} & y_{\mathrm{Nb}}^{\mathrm{s1}} y_{\mathrm{Va}}^{\mathrm{s2}}\,{}^{o}G_{\mathrm{Nb:Va}}^{\mathrm{BCC}} + y_{\mathrm{Nb}}^{\mathrm{s1}} y_{\mathrm{B}}^{\mathrm{s2}}\,{}^{o}G_{\mathrm{Nb:B}}^{\mathrm{BCC}} + 3RT\left[y_{\mathrm{B}}^{\mathrm{s2}}\ln\left(y_{\mathrm{B}}^{\mathrm{s2}}\right)\right. \\ & \left. + y_{\mathrm{Va}}^{\mathrm{s2}}\ln\left(y_{\mathrm{Va}}^{\mathrm{s2}}\right)\right] + y_{\mathrm{B}}^{\mathrm{s2}} y_{\mathrm{Va}}^{\mathrm{s2}}\left[{}^{0}L_{\mathrm{Nb:B,Va}}^{\mathrm{BCC}}\right. \\ & \left. + {}^{1}L_{\mathrm{Nb:B,Va}}^{\mathrm{BCC}}\left(y_{\mathrm{B}}^{\mathrm{s2}} - y_{\mathrm{Va}}^{\mathrm{s2}}\right) + \cdots\right] \end{aligned} \tag{7}$$

where $^{o}G_{\mathrm{Nb:Va}}^{\mathrm{BCC}}$ and $^{o}G_{\mathrm{Nb:B}}^{\mathrm{BCC}}$ correspond to:

$$\begin{aligned} {}^{o}G_{\mathrm{Nb:Va}}^{\mathrm{BCC}} &= {}^{o}G_{\mathrm{Nb}}^{\mathrm{BCC}} + 3\,{}^{o}G_{\mathrm{Va}} + \Delta_{\mathrm{f}}\,{}^{o}G_{\mathrm{Nb:Va}}^{\mathrm{BCC}} \\ {}^{o}G_{\mathrm{Nb:B}}^{\mathrm{BCC}} &= {}^{o}G_{\mathrm{Nb}}^{\mathrm{BCC}} + 3\,{}^{o}G_{\mathrm{B}}^{\mathrm{Rhom}} + \Delta_{\mathrm{f}}\,{}^{o}G_{\mathrm{Nb:B}}^{\mathrm{BCC}} \end{aligned} \tag{8}$$

The BCC phase is described within the limits of $(\mathrm{Nb})(\mathrm{Va})_3$ and $(\mathrm{Nb})(\mathrm{B})_3$, which correspond to the pure BCC-Nb, when the interstitial sublattice is empty, and to the metastable compound BCC-NbB_3, when the interstitial sublattice is completely filled with B atoms. Therefore, the Gibbs energy of the first end-member compound, $^{o}G_{\mathrm{Nb:Va}}^{\mathrm{BCC}}$, corresponds to that of the pure component Nb, $^{o}G_{\mathrm{Nb}}^{\mathrm{BCC}}$.

2.4. Solution phase NbB_2

The NbB_2 phase exhibits a hexagonal structure (*hP*3, space group *P6/mmm*, prototype AlB_2) with two sublattices, with Nb and B atoms occupying 1a and 2d positions, respectively. As mentioned before, this phase shows an extensive homogeneity range (65−70 at% B) [5,7−9]. Post et al. [28] compared the structural characteristics of several diborides and proposed substitutional vacancies in both Nb and B positions as defect mechanisms to explain the homogeneity range of NbB_2. Muzzy et al. [29], while studying AlB_2-type, B-rich $(\mathrm{Mo,Zr})_xB_2$ by neutron diffraction, reported that the metal vacant positions would accommodate the excess of boron in its structure. More recently, Nunes et al. [9] investigated the homogeneity range of NbB_2, also by neutron diffraction experiments, and confirmed Post's hypothesis. Therefore, the model $(\mathrm{Nb,Va})_1(\mathrm{B,Va})_2$ was adopted for NbB_2 in the present work with its Gibbs energy described by the following equation:

$$\begin{aligned} G_{\mathrm{m}}^{\mathrm{NbB_2}} = {} & y_{\mathrm{Nb}}^{\mathrm{s1}} y_{\mathrm{B}}^{\mathrm{s2}}\,{}^{o}G_{\mathrm{Nb:B}}^{\mathrm{NbB_2}} + y_{\mathrm{Nb}}^{\mathrm{s1}} y_{\mathrm{Va}}^{\mathrm{s2}}\,{}^{o}G_{\mathrm{Nb:Va}}^{\mathrm{NbB_2}} + y_{\mathrm{Va}}^{\mathrm{s1}} y_{\mathrm{B}}^{\mathrm{s2}}\,{}^{o}G_{\mathrm{Va:B}}^{\mathrm{NbB_2}} \\ & + y_{\mathrm{Va}}^{\mathrm{s1}} y_{\mathrm{Va}}^{\mathrm{s2}}\,{}^{o}G_{\mathrm{Va:Va}}^{\mathrm{NbB_2}} + RT\left\{\left[y_{\mathrm{Nb}}^{\mathrm{s1}}\ln\left(y_{\mathrm{Nb}}^{\mathrm{s1}}\right) + y_{\mathrm{Va}}^{\mathrm{s1}}\ln\left(y_{\mathrm{Va}}^{\mathrm{s1}}\right)\right]\right. \\ & \left. + 2\left[y_{\mathrm{B}}^{\mathrm{s2}}\ln\left(y_{\mathrm{B}}^{\mathrm{s2}}\right) + y_{\mathrm{Va}}^{\mathrm{s2}}\ln\left(y_{\mathrm{Va}}^{\mathrm{s2}}\right)\right]\right\} + {}^{E}G_{\mathrm{Nb,Va:B,Va}}^{\mathrm{NbB_2}} \end{aligned} \tag{9}$$

where

$$\begin{aligned} {}^{o}G_{\mathrm{Nb:B}}^{\mathrm{NbB_2}} &= {}^{o}G_{\mathrm{Nb}}^{\mathrm{BCC}} + 2\,{}^{o}G_{\mathrm{B}}^{\mathrm{Rhom}} + \Delta_{\mathrm{f}}\,{}^{o}G_{\mathrm{Nb:B}}^{\mathrm{NbB_2}} \\ {}^{o}G_{\mathrm{Nb:Va}}^{\mathrm{NbB_2}} &= {}^{o}G_{\mathrm{Nb}}^{\mathrm{BCC}} + 2\,{}^{o}G_{\mathrm{Va}} + \Delta_{\mathrm{f}}\,{}^{o}G_{\mathrm{Nb:Va}}^{\mathrm{NbB_2}} \\ {}^{o}G_{\mathrm{Va:B}}^{\mathrm{NbB_2}} &= {}^{o}G_{\mathrm{Va}} + 2\,{}^{o}G_{\mathrm{B}}^{\mathrm{Rhom}} + \Delta_{\mathrm{f}}\,{}^{o}G_{\mathrm{Va:B}}^{\mathrm{NbB_2}} \\ {}^{o}G_{\mathrm{Va:Va}}^{\mathrm{NbB_2}} &= {}^{o}G_{\mathrm{Va}} + 2\,{}^{o}G_{\mathrm{Va}} + \Delta_{\mathrm{f}}\,{}^{o}G_{\mathrm{Va:Va}}^{\mathrm{NbB_2}} \end{aligned} \tag{10}$$

and the excess term is given as follows:

$$\begin{aligned} {}^{E}G_{\mathrm{Nb,Va:B,Va}}^{\mathrm{NbB_2}} = {} & y_{\mathrm{Nb}}^{\mathrm{s1}} y_{\mathrm{Va}}^{\mathrm{s1}} y_{\mathrm{B}}^{\mathrm{s2}}\,{}^{0}L_{\mathrm{Nb,Va:B,Va}}^{\mathrm{NbB_2}} + y_{\mathrm{Nb}}^{\mathrm{s1}} y_{\mathrm{Va}}^{\mathrm{s1}} y_{\mathrm{Va}}^{\mathrm{s2}}\,{}^{0}L_{\mathrm{Nb,Va:Va}}^{\mathrm{NbB_2}} \\ & + y_{\mathrm{Nb}}^{\mathrm{s1}} y_{\mathrm{B}}^{\mathrm{s2}} y_{\mathrm{Va}}^{\mathrm{s2}}\,{}^{0}L_{\mathrm{Nb:B,Va}}^{\mathrm{NbB_2}} + y_{\mathrm{Va}}^{\mathrm{s1}} y_{\mathrm{B}}^{\mathrm{s2}} y_{\mathrm{Va}}^{\mathrm{s2}}\,{}^{0}L_{\mathrm{Va:B,Va}}^{\mathrm{NbB_2}} \end{aligned} \tag{11}$$

In Eq. (10), $^{o}G_{\mathrm{Nb:Va}}^{\mathrm{NbB_2}}$ and $^{o}G_{\mathrm{Va:B}}^{\mathrm{NbB_2}}$ correspond to the Gibbs energy of pure Nb and B with hexagonal *hp*3 structure, respectively.

Table 2
Optimized Gibbs energy coefficients for all phases of the Nb−B system

Phase	Model	Parameter	Coefficient		
			a	*b*	*c*
L	(Nb,B)	${}^{0}L^{\mathrm{L}}_{\mathrm{Nb,B}}$	−158 000	+19.5	
		${}^{1}L^{\mathrm{L}}_{\mathrm{Nb,B}}$	−21 500		
		${}^{2}L^{\mathrm{L}}_{\mathrm{Nb,B}}$	+147 500		
BCC	(Nb)(B,Va)$_3$	$\Delta_{\mathrm{f}}{}^{o}G^{\mathrm{BCC}}_{\mathrm{Nb:B}}$	+20 000		
		${}^{0}L^{\mathrm{BCC}}_{\mathrm{Nb:B,Va}}$	−74 000		
Nb_3B_2	$(Nb)_3(B)_2$	$\Delta_{\mathrm{f}}{}^{o}G^{\mathrm{Nb_3B_2}}_{\mathrm{Nb:B}}$	−295 300	−24.4	+6.65
NbB	(Nb) (B)	$\Delta_{\mathrm{f}}{}^{o}G^{\mathrm{NbB}}_{\mathrm{Nb:B}}$	−128 150	−7.7	+1.75
Nb_5B_6	$(Nb)_5(B)_6$	$\Delta_{\mathrm{f}}{}^{o}G^{\mathrm{Nb_5B_6}}_{\mathrm{Nb:B}}$	−727 900	−73.6	+14.0
Nb_3B_4	$(Nb)_3(B)_4$	$\Delta_{\mathrm{f}}{}^{o}G^{\mathrm{Nb_3B_4}}_{\mathrm{Nb:B}}$	−469 900	−65.3	+11.34
NbB_2	(Nb,Va) (B,Va)$_2$	$\Delta_{\mathrm{f}}{}^{o}G^{\mathrm{NbB_2}}_{\mathrm{Nb:B}}$	−196 200	+7.54	+0.25
		$\Delta_{\mathrm{f}}{}^{o}G^{\mathrm{NbB_2}}_{\mathrm{Va:B}}$	+100 416	−19.412	
		$\Delta_{\mathrm{f}}{}^{o}G^{\mathrm{NbB_2}}_{\mathrm{Nb:Va}}$	+10 000	+2.4	
		${}^{0}L^{\mathrm{NbB_2}}_{\mathrm{Nb,Va:B}}$	−106 000	+33.0	
		${}^{0}L^{\mathrm{NbB_2}}_{\mathrm{Nb:B,Va}}$	+180 000		
		${}^{0}L^{\mathrm{NbB_2}}_{\mathrm{Va:B,Va}}$	+200 000		
		${}^{0}L^{\mathrm{NbB_2}}_{\mathrm{Nb,Va:Va}}$	+200 000		

2.5. *Stoichiometric phases*

The crystal structures of the stoichiometric borides (Table 1) suggest the use of multiple sublattices for their modeling, as follows: (1) for Nb_3B_2, $(Nb)_2(Nb)_4(B)_4$; (2) for NbB, $(Nb)_4(B)_4$; (3) for Nb_5B_6, $(Nb)_2(Nb)_4(Nb)_4(B)_4(B)_4(B)_4$; and (4) for Nb_3B_4, $(Nb)_2(Nb)_4(B)_4(B)_4$. However, in the present work, positions occupied by the same element were considered energetically equivalent, reducing their description to 2-sublattices, using the smallest integers as stoichiometric indices. For each stoichiometric phase, there is only one possible arrangement

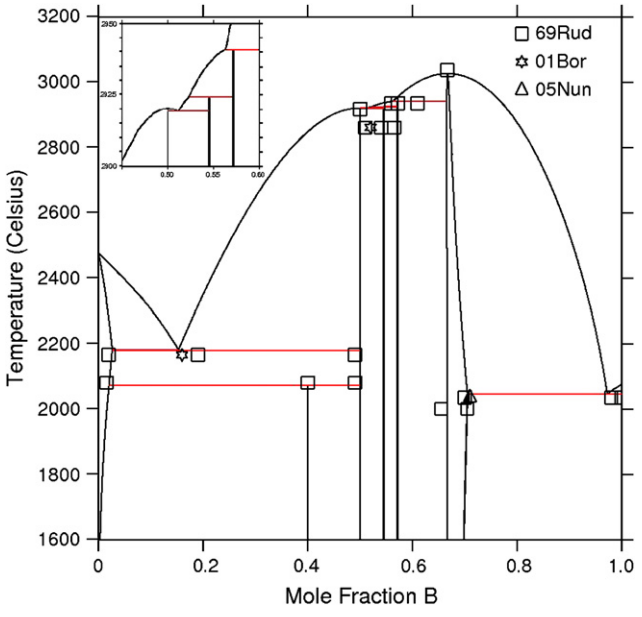

Fig. 3. Phase diagram of the Nb−B system calculated with the coefficients of the present work.

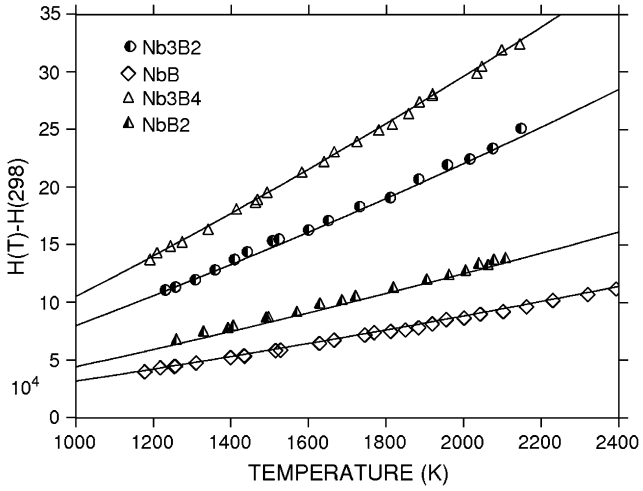

Fig. 4. Calculated enthalpy differences $[H(T) - H(298)]$ (continuous lines) for Nb_3B_2, NbB, Nb_3B_4 and NbB_2 and the values measured by Bolgar et al. [20] (symbols).

of the pure elements in the crystal structure of the compound. Therefore, the ideal and excess contributions to their Gibbs energies are equal to zero, leading to the following expressions for their Gibbs energies:

Nb_3B_2

$$G^{\mathrm{Nb_3B_2}}_{\mathrm{m}} = 3{}^{o}G^{\mathrm{BCC}}_{\mathrm{Nb}} + 2{}^{o}G^{\mathrm{Rhom}}_{\mathrm{B}} + \Delta_{\mathrm{f}}{}^{o}G^{\mathrm{Nb_3B_2}}_{\mathrm{Nb:B}} \quad (12)$$

NbB

$$G^{\mathrm{NbB}}_{\mathrm{m}} = {}^{o}G^{\mathrm{BCC}}_{\mathrm{Nb}} + {}^{o}G^{\mathrm{Rhom}}_{\mathrm{B}} + \Delta_{\mathrm{f}}{}^{o}G^{\mathrm{NbB}}_{\mathrm{Nb:B}} \quad (13)$$

Nb_5B_6

$$G^{\mathrm{Nb_5B_6}}_{\mathrm{m}} = 5{}^{o}G^{\mathrm{BCC}}_{\mathrm{Nb}} + 6{}^{o}G^{\mathrm{Rhom}}_{\mathrm{B}} + \Delta_{\mathrm{f}}{}^{o}G^{\mathrm{Nb_5B_6}}_{\mathrm{Nb:B}} \quad (14)$$

Nb_3B_4

$$G^{\mathrm{Nb_3B_4}}_{\mathrm{m}} = 3{}^{o}G^{\mathrm{BCC}}_{\mathrm{Nb}} + 4{}^{o}G^{\mathrm{Rhom}}_{\mathrm{B}} + \Delta_{\mathrm{f}}{}^{o}G^{\mathrm{Nb_3B_4}}_{\mathrm{Nb:B}} \quad (15)$$

Table 3
Enthalpies of formation at 298.15 K for the stable Nb-borides

Phase	Enthalpy at 298.15 K (kJ/mol of phase)	
	Calculated	Experimental
Nb_3B_2	−298	–
NbB	−128.7	–
Nb_5B_6	−723.1	–
Nb_3B_4	−473.3	–
NbB_2	−196.3	−175 ± 7.5 [15] −245 ± 6 [16] −186 ± 18 [17] −213 ± 3 [18] −180 ± 4.5 [19]

Table 4
Entropies at 298.15 K for the stable Nb-borides

Phase	Entropy at 298.15 K (kJ/mol of phase. K)	
	Calculated	Experimental
NbB_2	38.7	38.1 [13]
Nb_3B_2	99.4	102.0 [14]
NbB	38.1	38.0 [14]
Nb_5B_6	196.5	–
Nb_3B_4	121.7	121.1 [14]

3. Optimization procedure (results and discussion)

The ${}^{n}L_{ij}^{\phi}$ parameters in Eqs. (6), (7) and (11) ($\phi = $ L, BCC or NbB_2) as well as the Gibbs energy of formation of the end-members in Eqs. (8) and (10) and of the stoichiometric compounds in Eqs. (12)−(15) are described according to Eq. (5). Their coefficients a, b and c correspond to the adjustable variables in the optimization procedure (see Table 2).

The temperature dependent Gibbs energies of the pure elements in their stable and metastable states were taken from SGTE database [30] and are given in Appendix.

The model $(Nb)_1(B,Va)_3$ chosen for the BCC leads to the definition of the end-member NbB_3, with its Gibbs energy of formation given by $\Delta_f {}^{o}G_{Nb:B}^{BCC}$, for which no experimental value is available. A positive value of 5000 J/mol of atoms has been often used, e.g. Ref. [31], for the Gibbs energy of formation of such metastable compounds, thus, a value of 20 000 J/mol of phase was adopted here for $\Delta_f {}^{o}G_{Nb:B}^{BCC}$.

The SGTE descriptions for hcp-Nb and hcp-B were adopted for the parameters $\Delta_f {}^{o}G_{Nb:Va}^{NbB_2}$ and $\Delta_f {}^{o}G_{Va:B}^{NbB_2}$ in Eq. (10), respectively. The Gibbs energy of the end-member with vacancies in both sublattices of the phase NbB_2 was assumed to be zero (${}^{o}G_{Va:Va}^{NbB_2} = 0$).

The liquidus line and the temperatures of the invariant reactions measured by Rudy and Windisch [5] with the modifications proposed in Refs. [10,11] were adopted in the optimization procedure. However, to make the stability of Nb_5B_6 compatible with the measurements of Rudy and Windisch, the 3133 K reported for the eutectic L ↔ NbB + Nb_3B_4 was assumed to be valid for the eutectic L ↔ NbB + Nb_5B_6, with the composition of the liquid at 52 at% B [10]. The temperature for the peritectic formation of Nb_5B_6 (L + Nb_3B_4 ↔ Nb_5B_6) was assumed to be 3170 K, which is a mean value between the temperatures given by Rudy and Windisch for the immediate neighbor invariant transformations. Furthermore, all thermodynamic data available were used in the optimization procedure.

The optimized Gibbs energy coefficients for the phases of the Nb−B system are presented in Table 2. The calculated phase diagram is shown in Fig. 3, where a good agreement between the experimental and calculated values can be observed. The calculated enthalpy differences, $H(T) - H(298)$, for the phases Nb_3B_2, NbB, Nb_3B_4 and NbB_2 reproduce well the values measured by Bolgar et al. [20], as shown in Fig. 4. The calculated and experimental data for the enthalpies and the entropies of the intermediate compounds at 298.15 K are compared in Tables 3 and 4, respectively, also showing a good agreement.

Acknowledgements

The authors gratefully acknowledge the financial support of FAPESP through grants #97/06348-4 (Nb−B−Si), #99/06160-0, and #00/08062-5.

Appendix: Gibbs energies of the pure elements in their stable and metastable states (in J/mol).

$${}^{o}G_{Nb}^{BCC} = -8519.353 + 142.045475T - 26.4711T\ln(T) + 2.03475e^{-4}T^2 - 3.5012e^{-7}T^3 + 93399T^{-1} \quad (298.13 < T < 2750)$$

$${}^{o}G_{Nb}^{BCC} = -37\,669.3 + 271.720843T - 41.77T\ln(T) + 1.528238e^{+32}T^{-9} \quad (2750 < T < 6000)$$

$${}^{o}G_{B}^{Rhom} = -7735.284 + 107.111864T - 15.6641T\ln(T) - 0.006864515T^2 + 6.18878e^{-7}T^3 + 370843T^{-1} \quad (298.13 < T < 1100)$$

$${}^{o}G_{B}^{Rhom} = -16649.474 + 184.801744T - 26.6047T\ln(T) - 7.9809E-04T^2 - 2.556e^{-8}T^3 + 1748\,270T^{-1} \quad (1100 < T < 2348)$$

$${}^{o}G_{B}^{Rhom} = -36667.582 + 231.336244T - 31.5957527T\ln(T) - 0.00159488T^2 + 1.34719e^{-7}T^3 + 11205883T^{-1} \quad (2348 < T < 3000)$$

$${}^{o}G_{B}^{Rhom} = -21530.653 + 222.396264T - 31.4T\ln(T) \quad (3000 < T < 6000)$$

$${}^{o}G_{B}^{L} = +29781.555 - 10.816418T - 3.06098e^{-23}T^7 + {}^{o}G_{Nb}^{BCC} \quad (298.13 < T < 2750)$$

$${}^{o}G_{B}^{L} = -7499.398 + 260.756148T - 41.77T\ln(T) \quad (2750 < T < 6000)$$

$${}^{o}G_{Nb}^{L} = +48458.559 - 20.268025T + {}^{o}G_{B}^{Rhom} \quad (298.13 < T < 500)$$

$${}^{o}G_{Nb}^{L} = +41119.703 + 82.101722T - 14.9827763T\ln(T) \quad (500 < T < 2348)$$

$${}^{o}G_{Nb}^{L} = -0.007095669T^2 + 5.07347e^{-7}T^3 + 335484T^{-1} \quad (2348 < T < 3000)$$

$${}^{o}G_{Nb}^{L} = +28842.012 + 200.94731T - 31.4T\ln(T) \quad (3000 < T < 6000)$$

$${}^{o}G_{Nb}^{L} = +50372.665 - 21.448954T + {}^{o}G_{B}^{Rhom}$$

$${}^{o}G_{Nb}^{HCP} = +10000 + 2.4T + {}^{o}G^{Bcc,Nb} \quad (298.13 < T < 6000)$$

$${}^{o}G_{B}^{HCP} = +100416 - 19.412T + 2{}^{o}G^{Rhomb,B} \quad (298.13 < T < 6000)$$

References

[1] Bewlay BP, Jackson MR, Zhao J-C, Subramanian PR. Metallurgical and Materials Transactions A 2003;34:2043−52.

[2] Zhao J-C, Westbrook JH. MRS Bulletin 2003;28:622−30.

[3] Massalski TB, editor. Binary alloy phase diagrams. 2nd ed., 3 vols.. Materials Park, OH: ASM International; 1990.

[4] Nowotny H, Benesovsky F, Kieffer R. Zeitschrift für Metallkunde 1959;50:417−23.

[5] Rudy E, Windisch St. Ternary phase equilibria in transition metal−boron−carbon−silicon systems, AFML-TR-65-2, part I, vol. X. OH: Wright-Patterson Air Force Base; 1966.

[6] Bolmgren H, Lundstroem T. Journal of the Less-Common Metals 1990; 159:L25−7.

[7] Nowotny H, Benesovsky F, Rudy E, Wittmann A. Monatshefte für Chemie 1960;91:975−90.

[8] Rudy E, Benesovsky F, Toth L. Zeitschrift für Metallkunde 1963; 54:345−53.

[9] Nunes CA, Kaczorowski D, Rogl P, Baldissera MR, Suzuki PA, Coelho GC, et al. Acta Materialia 2005;53:3679−87.

[10] Borges Jr. LA. MSc. thesis, FAENQUIL, Brazil; 2001.

[11] Borges Jr LA, Coelho GC, Nunes CA, Suzuki PA. Journal of Phase Equilibria 2003;24:140−6.

[12] Glaser FW. Transactions of the American Institute of Mining and Metallurgical Engineers 1952;194:391−6.

[13] Westrum EF, Clay GA. Journal of Physical Chemistry 1963;67:2385−7.

[14] Blinder AV, Bolgar AS. Soviet Powder Metallurgy and Metal Ceramics 1991;30:1053−6.

[15] Huber Jr. EJ. 5th Quarterly report, AVCO-SR-63-183; 1963.

[16] Johnson GK, Greenberg E, Margrave JL, Hubbard WN. Journal of Chemical and Engineering Data 1967;12:597−600.

[17] Reznitskii LA. Russian Journal of Physical Chemistry 1967;41:612−4.

[18] Kirpichev EP, Rubtsov YuI, Sorokina TV, Prokudina VK. Russian Journal of Physical Chemistry 1979;53:1128−30.

[19] Meschel SV, Kleppa OJ. Metallurgical Transactions A 1993;24:947−50.

[20] Bolgar AS, Serbova MI, Serebryakova TI, Isaeva LP, Fesenko VV. Soviet Powder Metallurgy and Metal Ceramics 1983;243:57−62.

[21] Kaufman L, Uhrenius B, Birnie D, Taylor K. CALPHAD 1984;8:25−66.

[22] Sundman B, Ågren J. Journal of Physics and Chemistry of Solids 1981;42:297−301.

[23] Hillert M. The compound energy formalism. Journal of Alloys and Compounds 2001;320:161−76.

[24] Villars P, Calvert LD. Pearson's handbook of crystallographic data for intermetallic phases. 2nd ed., 4 vols.. Materials Park, OH: ASM International; 1991.

[25] Bolmgren H, Lundström T, Tergenius L-E. Journal of the Less-Common Metals 1990;161:341−5.

[26] Redlich O, Kister AT. Journal of Industrial and Engineering Chemistry 1948;40:345−8.

[27] Kiessling R. Acta Chemica Scandinavica 1949;3:603−15.

[28] Post B, Glaser FW, Moskowitz D. Acta Metallurgica 1954;2:20−5.

[29] Muzzy LE, Avdeev M, Lawes G, Haas MK, Zandbergen HW, Ramirez AP, et al. Physica C 2002;382:153−65.

[30] Dinsdale AT. CALPHAD 1991;15:317−425.

[31] Neto JGC, Fries SG, Lukas HL, Gama S, Effenberg G. CALPHAD 1993;17:219−28.